Key Engineering Materials Vols. 280-283 (2005) pp. 1909-1912
online at http://www.scientific.net

2005-SMF-0506

Raman Spectra Study on Multilayered Compositional Graded $(Ba_{0.8}Sr_{0.2})(Ti_{1-x}Zr_x)O_3$ Thin Films

Can Wang, B.L. Cheng*, S.Y. Wang, S. Y. Dai, and Z.H. Chen

Institute of Physics, Chinese Academy of Sciences, Beijing 100080, P.R. China

Keywords: Raman spectra, Multilayered thin film, Compositional graded layer

Abstract. Compositional graded thin films of $(Ba_{0.8}Sr_{0.2})(Ti_{1-x}Zr_x)O_3$ (BSTZ) are grown on MgO by pulsed laser deposition technique with four BSTZ ceramic targets. Gradients of composition are achieved by artificially tailoring composition in multilayered thin films to form compositional graded layers (CGL). In each CGL four individual layers of BSTZ with x = 0.36, 0.18, 0.08 and 0 are grown in series with equal thickness. Three kinds of CGL samples comprising one, two or four CGLs have been elaborated with the same total thickness by varying the thickness of each CGL. Raman spectra show existence of tetragonal structure in all the multilayered BSTZ thin films. Raman peak at 535 cm^{-1} shifts to high frequency with increasing of compositional gradient, and the peak at 750 cm^{-1} also shows a small shift to high frequency. Moreover, other Raman peak is observed at about 830 cm^{-1}, which is associated with phonon mode of cubic phase, and such peak shifts towards lower frequency with increasing of compositional gradient. The shift of Raman peak is related to variation of internal stress in BSTZ thin film due to increasing compositional gradient.

Introduction

Recently, ferroelectric films with a composition gradient normal to substrate plane have attracted much attention because of their remarkable properties like giant pyroelectric coefficient, polarization offset, high tunability, low temperature coefficient of dielectric constant, and low leakage current, etc, which may result from the gradients of polarization and internal stresses. Especially, dielectric properties of BST films with different Ba/Sr concentration gradients for tunable devices have been reported, and improved tunability and low temperature coefficient of dielectric constant have been observed on such compositionally graded BST thin films [1,2].

We have reported fabrication and characterization of BSTZ multilayered thin films with compositional graded layers grown on $Pt/TiO_2/SiO_2/Si$ and Nb doped $SrTiO_3$ substrates [3,4]. Improved dielectric permittivity, tunability and good temperature stability of permittivity have been observed in the compositional graded thin films. In these multilayered thin films, inevitably, internal stress induced by the gradient of composition should have an effect on microstructure and electric properties.

Stress has always been one of the major interests in the study of ferroelectric thin films. Film stresses, including thermal stress due to thermal expansion coefficient difference between film and substrate, intrinsic stress determined by growth parameters and extrinsic stress caused by structural changes, can significantly change mechanical, dielectric and optical properties and influence nature of phase transitions. Raman spectra as a nondestructive probe have been used for thin films characterization. Useful information about impurities, internal stress, and crystal symmetry can be obtained in various thin films. Raman studies have shown that, for $BaTiO_3$ thin films, compressive stress can cause red shift while the reverse is true for tensile stress [5,6].

To get more information about effects of gradient of composition on the microstructure and characterization of BSTZ thin films, Raman properties of BSTZ multilayered thin films have been investigated.

* Corresponding author: blcheng@aphy.iphy.ac.cn

Experiments

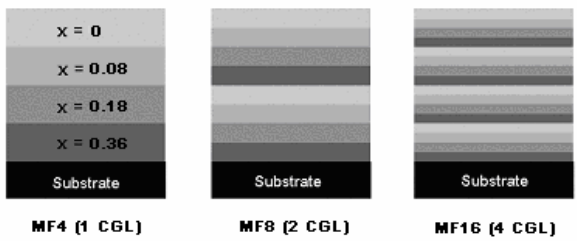

Fig. 1 Schematic configurations of multilayered $(Ba_{0.80}Sr_{0.20})(Ti_{1-x}Zr_x)O_3$ films with compositionally graded layer.

The graded multilayered BSTZ thin films have been grown on MgO substrates using a pulsed laser deposition technique. Four kinds of targets $(Ba_{0.80}Sr_{0.20})(Ti_{1-x}Zr_x)O_3$ (x =0.36, 0.18, 0.08, 0) (BSTZ), prepared by conventional solid-state reaction process, were mounted on motor-driving rotary stands. Thin films were deposited on MgO substrates at 550°C with oxygen pressure of 1 Pa. After deposition the sample was annealed in-situ at 550°C for 15 minutes under about 500 Pa oxygen pressure to reduce oxygen vacancies in the films. Individual layers were grown from the different targets orderly in vacuum in order to eliminate formation of any surface layers, which can extrinsically affect the film properties. The gradients of composition were achieved by varying the thickness of individual layer, but to keep the total thickness of all the films around 640 nm by the series of CGLs. Schematic of the final films were shown in Fig. 1, and the samples were signed as MF4, MF8, and MF16, respectively. In each CGL, four individual layers of BSTZ, with x = 0.36, 0.18, 0.08 and 0, respectively, were grown in series, and the thickness of the individual layer was about 160, 80, and 40 nm for the three samples, accordingly, by controlling of the number of laser pulses.

Crystallinity of the multilayered BSTZ thin films was examined by XRD with Cu *Kα* radiation. Raman scattering measurements were carried out at room temperature in backscattering geometry with a Jobin-Yvon T64000 triple Raman spectrometer. A 514.5 nm Ar^+ ion laser line was used for excitation with power of 100 mW. Incident light was perpendicular to the specimen surface. The spectrometer provided a wave number resolution of ~0.5 cm^{-1} and accuracy of ~0.1 cm^{-1}.

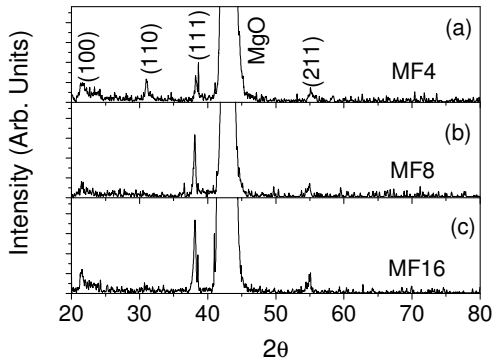

Fig. 2 XRD profile for the multilayered BSTZ films on MgO with different compositional gradient.

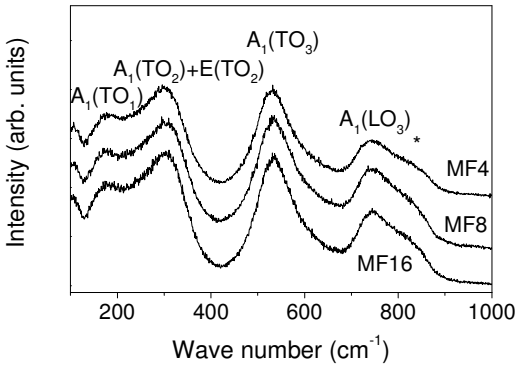

Fig. 3 Room temperature Raman spectra of BSZT multilayered thin films with different compositional graded layers.

Results and discussion

XRD profiles of the thin films on MgO are shown in Fig. 2, indicating that the multilayered thin films are crystallized into perovskite structure. Even there is a large lattice mismatch between thin film and MgO substrate, the crystallinity of the multilayered thin films is still reasonably well at relatively lower deposited temperature of 550 °C.

Fig. 3 shows Raman spectra for the BSTZ multilayered thin films. Optical phonons in bulk MgO are Raman inactive due to crystal symmetry, so the substrate should have no effect on the Raman signals of the thin films. It is known that, in paraelectric cubic phase of ABO_3 perovskite, there are 12 optical modes $(3F_{1u}+1F_{2u})$ which are not first-order Raman active. In tetragonal phase, each F_{1u} mode

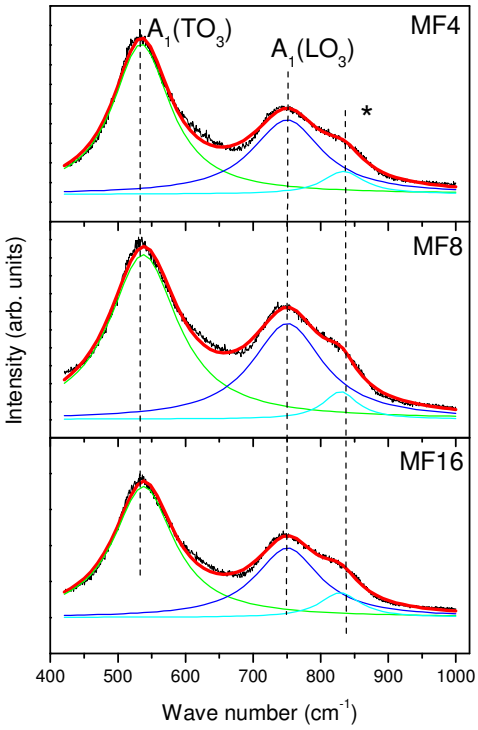

Fig. 4 Deconvolution of high frequency Raman spectra. Scattered points are experimental data, thick lines are fitted results, and the thin lines show Raman peaks. The dashed line is guide to eye.

splits into an A_1 mode and an E mode, while the F_{2u} mode splits into B_1 and E, resulting in $3A_1+B_1+4E$ modes. These modes further split into longitudinal (LO) and transverse (TO) modes due to long range of electrostatic forces associated with lattice ionicity. Then we obtain the following distinct Raman-active optical lattice vibrations for BTO in the tetragonal phase: $3A_1(TO) + 3A_1(LO) + 3E(TO) + 3E(LO) + 1E(LO+TO) + 1B_1$.

The main Raman peaks for BSTZ multilayered thin films, as shown in the Fig. 3, can be attributed to the $A_1(TO_1)$, $A_1(TO_2) + E(TO_2)$, $A_1(TO_3)$, and $A_1(LO_3)$, according to the Raman spectra for the tetragonal phase $BaTiO_3$ single crystal, which suggests the existence of tetragonal phase in the BSTZ multilayered thin films. Here, the subscripts 1, 2 and 3 of the TO and LO modes are used to label the Raman modes, where 1 refers to the lowest-frequency phonon and 3 refers to the highest-frequency phonon. Moreover, an additional peak marked by asterisk, which does not appear for $BaTiO_3$, is observed at about 830 cm^{-1}. This peak is similar to the optical phonons at 795 cm^{-1} (LO_4) for $SrTiO_3$ single crystal [7].

In our case, BSTZ films have different crystal structure depending on the Zr content. For single crystal BSTZ, the temperature of phase transition T_C (cubic to tetragonal phase) decreases, both T_2 (tetragonal to orthorhombic phase) and T_3 (orthorhombic to rhombohedral phase) increase with increasing Zr content. When the content of Zr larger than a critical value, all these three-phase transitions were merged together, and T_C decreases with increase in Zr content. The layers in the multilayered film have different Zr content, so there exist tetragonal phase layer for the layer with x=0, and cubic phase layer for the layer with x=0.36. Coexistence of different phases in the multilayered thin films can provide complicated phenomena in Raman spectra. Because of the existence of cubic phase layer with x=0.36 in the multilayered thin films, it is reasonable to ascribe the peak at 830 cm^{-1} to the LO_4 mode in cubic phase, and blue shift from 795 to 830 cm^{-1} should result from larger lattice constant of BSTZ than $SrTiO_3$.

To get more detail and accurate information from Raman spectra, high frequency Raman spectra were fitted by superposition of Lorentz peak expressed by formula as

$$I(\omega) = I_0 + \frac{2A}{\pi}\frac{W}{4(\omega-\omega_0)^2 + W^2} \quad (1)$$

where ω_0 is phonon frequency of the peak, W is its FWHM, A is a constant, and I_0 is intensity of the background. From fitting as shown in Fig. 4, the peak position of the three peaks is listed in Table 1.

Table 1 Peak position of high frequency optical modes of BSTZ mutilayered thin films

Sample	$A_1(TO_3)$ (cm^{-1})	$A_1(LO_3)$ (cm^{-1})	(LO_4) (cm^{-1})
MF4	534.6	750.0	833.8
MF8	537.5	750.8	829.2
MF16	537.9	750.6	828.5

According to the fitted value shown in Table 1, Raman mode of $A_1(TO_3)$ shifts to high frequency with increasing of compositional gradient, and $A_1(LO_3)$ also has a little shift to high frequency. The blue shift of the two Raman peaks suggests the tetragonal layer in the multilayered thin films suffer a tensile stress that increases with increasing compositional gradient. Moreover, Raman mode of LO_4, resulting from the optical phonons mode from cubic phase, shifts towards lower frequency with increasing compositional gradient, which indicates that compressive stress in the layer of cubic phase is increased with compositional gradient.

In BSTZ materials, due to the ionic radius of Zr^{+4} larger than that of Ti^{+4}, the lattice parameter increases with increasing Zr content. Therefore, the lattice parameter for the individual layers is not equal. The layer for x = 0 with a smallest lattice parameter should suffer a tensile stress, and the layer for x = 0.36 with a larger lattice parameter should suffer a compressive stress in the samples of MF8 and MF16 except for the first layer on the MgO substrate. The first layer for x = 0.36 on MgO in all the three samples is suffer a tensile stress because the MgO substrate has larger parameter than BSTZ. With the decrease of the thickness of individual layer (increase of the compositional gradient), both the stresses increase, then the lattice constant for the layer of x = 0.36 should be decreased and that for the layer of x=0 should be increased. The variation of lattice constant for individual layers described as above has been evidenced by the XRD results on BSTZ multilayered thin films grown on Pt [3].

As a conclusion, the blue shift of the Raman frequency for the tetragonal phase layer is related to the increase of tensile stress, and the red shift of the Raman frequency for the cubic phase layer is related to the increase of compressive stress with the increase of compositional gradient. Furthermore, Raman shift provides evidence of modulation of stress in BSTZ multilayered thin films.

Acknowledgements

The authors are very grateful for the financial support of the ‘‘Hundreds Talents Project’’ of the Chinese Academy of Sciences, the Chinese Postdoctoral Science Foundation, and National Natural Science Foundation of China.

References

[1] S. G. Lu, X. H. Zhu, C. L. Mak, K. H. Wong, H. L. W. Chan, and C. L. Choy: Appl. Phys. Lett. Vol. 82 (2003), pp.2877.
[2] X. H. Zhu, N. Chong, H. Lai-Wah Chan, C. L. Choy, K. H. Wong, Z. G. Liu, and N. B. Ming: Appl. Phys. Lett. Vol. 80 (2002), pp.3376.
[3] C. Wang, B.L. Cheng, S.Y. Wang, H.B. Lu, Y.L. Zhou, Z.H. Chen and G.Z. Yang: Appl. Phys. Lett. Vol. 84 (2004), pp.765.
[4] B.L. Cheng, C. Wang, S.Y. Wang, T. W. Button, H.B. Lu, Y.L. Zhou, Z.H. Chen and G.Z. Yang: submitted to Appl. Phys. Lett. (2004)
[5] S. B. Desu: Phys. Status Solidi a, Vol. 141 (1994), pp.119
[6] J. S. Zhu, X. M. Lu, W. Jiang, W. Tian, M. Zhu, M. S. Zhang, X. B. Chen, X. Liu and Y. N. Wang: J. Appl. Phys. Vol. 81 (1997), pp. 1392.
[7] H. Vogt and G. Rossbroich: Phys. Rev. B, Vol. 24 (1981), pp. 3086.